Heat and Mass Transfer (2019) 55:2025–2036
https://doi.org/10.1007/s00231-018-2491-3

ORIGINAL

Numerical study of chemical kinetics and radiation heat transfer characteristics on the temperature distribution in the oxy-fuel combustion

E. Ebrahimi Fordoei [1] · Kiumars Mazaheri [1]

Received: 2 February 2018 / Accepted: 26 September 2018 / Published online: 5 November 2018

Abstract

In this study, The IFRF methane-oxygen combustion furnace is used to investigate the effect of the radiation model, the method of evaluated absorption and emission coefficients and the different chemical mechanisms. The simulations are performed with OpenFOAM open source software by using of PaSR (partially stirred reactor) combustion model. The numerical investigations are carried out without radiative heat transfer and with the modeling of the radiation source term using the P1 (spherical harmonic radiation model) and DO (discrete ordinate) models. To evaluate the absorption and emission coefficients used from the constant coefficients, the grey mean gases model in terms of temperature polynomial, the WSGGM (weighted sum of grey gases model) and refined WSGGM models. The investigation of the global mechanism effect on the temperature distribution in the oxy-fuel combustion is performed by the modified 2-step Westbrook-Dryer mechanism by Yin and modified 4-step Jones-Lindstedt mechanisms by Yin and Andersen. The results indicate that the lack of consideration of radiation heat transfer in the oxy-fuel combustion leads to a large error in the prediction of the maximum and average temperature distributions inside the furnace. Also, the DO model has less error than P1 model due to more heat loss prediction by P1 model in the low optical thickness. The WSGGM model for calculating of absorption and emission coefficients provide the best result in comparison with other methods. The refined 4-step Jones-Lindstedt mechanism by Andersen has best prediction of on the basis of numerical simulations.

Abbreviations

CCS	Carbon capture and storage
CFD	Computational fluid dynamic
DO	Discrete ordinate
IFRF	International Flame Research Foundation
JL	Jones-Lindstedt
NG	Natural gas
P1	Harmonic radiative heat transfer model
PaSR	Partially stirred reactor
PDE	Partially differential equation
PISO	Pressure-implicit with splitting of operators
RTE	Radiative transfer equation
SIMPLE	Semi-implicit method for pressure-linked equations
WD	Westbrook-Dryer
WSGGM	Weighted sum of grey gases model

✉ Kiumars Mazaheri
Kiumars@modares.ac.ir

[1] Department of Mechanical Engineering, Tarbiat Modares University, Tehran, Iran

1 Introduction

Combustion systems using fossil fuels are the main source of energy in industrial systems. The important issues associated with these systems are increased efficiency, reduced pollution and greenhouse emissions [1]. Oxy-fuel combustion has been proposed as one of the new ways to increase the efficiency of combustion systems while reducing emissions of environmental pollutants in recent years [2]. The pure oxygen is used as the oxidizer in oxy-fuel combustion. This makes the combustion products different from the air-fired combustion conditions. Combustion products mainly consist of CO_2 and H_2O due to the use of pure oxygen in oxy-fuel combustion. Thus, carbon dioxide is separated from water vapor using the condensation process, and it is possible to the carbon capture and storage (CCS) of CO_2 which is the main source of greenhouse gases [3, 4].

In the oxy-fuel combustion, the temperature is much higher than the air-fuel combustion due to the replacement of N_2 with O_2. The increase in the temperature leads to more radical production, which is not predicted by reduced and global kinetics and can lead to errors in the calculation of temperature and species distributions [5, 6]. Regarding this issue, various

studies have been done to improve the global chemical kinetics in order to use in oxy-fuel combustion. The 3-step and 6-step kinetics (modified two step Westbrook-Dryer (WD) [7] and four step Jones-Lindstedt (JL) [8] kinetics) was first proposed by Andersen et al. [9] for use in oxy-fuel combustion. In this kinetics, the coefficients and reactions are modified to be capable of being used in the combustion with different oxygen concentrations. The results obtained from this kinetics were compared with the experimental data using a counter flow diffusion flame solver. The conformance and acceptable accuracy of refined kinetics were observed in a wide range of oxygen concentrations with experimental data. Yin et al. [10] modified the 2-step WD and 4-step JL chemical kinetics for use in methane-oxygen combustion. In this study, one and two step reactions were added to WD and JL kinetics, respectively. Also, Yin et al. [10] corrected the reaction coefficients to use of them in the oxy-fuel combustion. Modified chemical kinetics showed a much better accuracy than the initial kinetics (the distribution of carbon monoxide in the furnace by using modified kinetics is about 50% more accurate than the original kinetics).

In the oxy-fuel combustion to reduce the maximum and average temperature in order to increase its applications in various industries, the mixing of oxygen with combustion products, especially CO_2 and H_2O is used. Lei et al. [11] carried out the computational fluid dynamics (CFD) simulations of a swirling diffusion flame under air-fired and oxy-fuel conditions. This study was conducted with O_2/CO_2 mixture as oxidizer. The eddy dissipation and eddy dissipation concept models has been used with quasi-global and global kinetic mechanisms in this study. Results show that reasonable CO predictions can only be obtained using a finite-rate approach with appropriate mechanisms considering the CO_2 chemical effects. The WD 2-step mechanism consistently underestimates the CO concentrations. In contrast, the multiple-step mechanism captures the chemical effects of CO_2, and improves the predictions.

Another important aspect is the modeling of radiative heat transfer in reactive flow simulations. Radiative heat transfer is very important due to the high temperature of combustion gases. Furthermore, the carbon dioxide and water vapor have the major contribution to radiation heat transfer in combustion process because these species have high absorption and emission coefficients [12, 13]. Oxy-fuel combustion strongly promotes radiative heat transfer, as a result of the much higher levels of CO_2, H_2O. There are two important matter for the correct prediction of radiation heat transfer: radiation model and the calculation of absorption and emission coefficients. Yin et al. [10, 14, 15] modified the weighted sum of grey gases model (WSGGM) presented by Smith [16] to calculate the absorption and emission coefficients in oxy-fuel combustion. The modified model was used to simulate a 1 MW laboratory furnace and a 609 MW utility boiler. The results show that the modified WSGGM model is not significantly different from that of the WSGGM model in the laboratory furnace, while it shows a significant difference in the utility boiler. The results of modified WSGGM model has significant improvement in the result of actual boiler. The non-grey gases radiation effect and comparison of it with grey gases method in oxy-fuel combustion done by Wheaton et al. [17]. All simulation conditions are considered similar in this investigation. There was a very small difference in the prediction of temperature and species distributions by using two models, while simulation time is assumed to be higher by assumption of non-grey gases. The experimental study of radiation characteristics on the combustion with O_2/CO_2 mixture (oxy-fuel combustion) and air done by Andersen et al. [18]. The experiments were carried out in a test furnace with real flue gas recycle for creation of O_2/CO_2 combustion. The obtained results from the radiation characteristics and temperature profiles showed the emissivity of hot combustion products for the oxy-fuel combustion differ from air-fired combustion. The total emissivity and the gas emissivity were very different for the O_2 and CO_2 volume fraction equal to 27 and 73%, respectively with the air-fired environment.

According to the mentioned contents, the chemical mechanism and the radiative heat transfer characteristics are different in the oxy-fuel combustion in comparison with air-fired combustion. The chemical mechanism affects on the reaction rates, species production and consumption. The different combustion models can exhibit various behaviors in the prediction of temperature and species distributions with different chemical kinetics. Furthermore, different species distributions (especially CO_2 and H_2O concentrations) affect the radiation heat transfer calculations. Therefore, the effect of the different chemical mechanisms and radiative heat transfer characteristics is examined by using of PaSR combustion model to simulate oxy-fuel combustion in the present study (this model was not used for the turbulence-combustion interaction modelling in other studies [10, 14, and 15]). The effect of the applying radiation (not investigated in other studies), radiation model, and the method of calculating the absorption and emission coefficients are taken into consideration for the radiation heat transfer effect on the oxy-fuel combustion simulation. Also, 2-step and 4-step global kinetics developed for the oxy-methane combustion are investigated with PaSR combustion model.

2 Computational details

2.1 Furnace configuration

The oxy-fuel combustion furnace has 0.88 MW thermal power and the burners are high velocity. The furnace is developed and tested in the OXYFLAM2 project at the IFRF [19, 20].

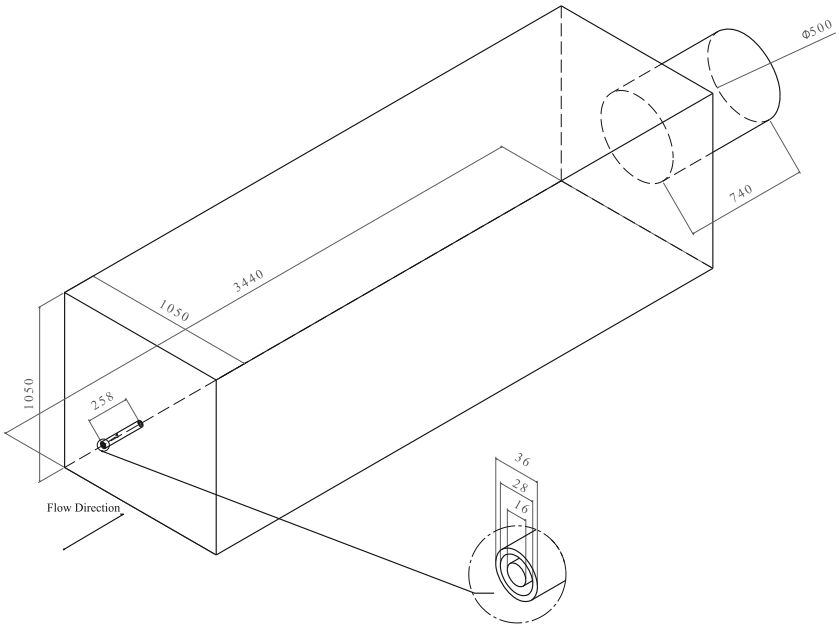

Fig. 1 IFRF furnace geometry and dimensions (in mm)

The configuration of the IFRF furnace and its dimensions are shown in Fig. 1. According to Fig. 1, the length of the furnace is 3440 mm, which has a square cross section with dimensions of 1050 mm. At the end of the furnace, a chimney with 740 mm length and 500 mm diameter is considered for the exhaust of combustion products. The burners include two different inputs. The central portion of the burner has 16 mm diameter where the natural gas (NG) is flowing. Also, an annular section with internal diameter of 28 mm and outer diameter of 36 mm is considered for oxidizer inlet. The length of the fuel and oxidizer inlet pipes is 258 mm.

The quarter of the geometry considered in this study due to geometrical and physical symmetries (which can be seen with great approximation in the results of experimental data [20]), and in order to reduce the volume of numerical computation costs.

2.2 Governing conditions on the furnace

Natural gas and oxygen are used as fuel and oxidizer respectively in the furnace. The analysis of the NG shows that the fuel composition is assumed to be in accordance with Table 1 [20, 21]. NG contains various percentages of hydrocarbons in which the major part is methane (86% of the total 94% of the hydrocarbons in the NG). Also, 6% of the NG is N_2, CO_2 and O_2. Hence, the share of other high carbon hydrocarbons which is about 8%, is dedicated to methane. Since oxygen accounts for more than 99.5% of the oxidizer (Table 2), pure oxygen is used as oxidizer [15, 16].

Different boundary conditions governing the fuel and oxidizer inlets including mass flow rates, velocity, temperature and pressure, are presented in Table 3. The pressure 30 (Pa) was generated to prevent air leakage into the furnace which is also considered in numerical simulation. Other boundary conditions are shown in Fig. 2. The numerical domain has two symmetry planes that gradient of all quantities are zero in these planes. The temperature profile of the upper and side walls are according to the experimental data given in references [20, 21], has been applied deduced using Eq. 1. In the Eq. 1, z represents the axial distance from the beginning of the furnace in meters.

$$T(z) = 1700{\cdot}598 + 212{\cdot}5872z - 46{\cdot}66929z^2\ [K] \quad (1)$$

For the primary and end walls of the furnace, which are in the vicinity of fuel and air entry nozzles and chimneys respectively, the boundary condition of the insulation wall is used in accordance with experimental conditions. The wall emissivities are used from Bollettini et al. [21]. The constant pressure boundary condition is considered for the outlet of the furnace. It should be noted that the flow boundary condition for all walls is considered as no slip condition.

Table 1 Mole fraction of different species of fuel and its properties

Species	CH_4	C_2H_6	C_3H_8	C_4H_{10}	C_5H_{12}	CO_2	N_2	O_2
NG volume fraction	86	5.4	1.87	0.58	0.14	1.79	4.01	0.21
Molecular weight fuel	Density in standard pressure and temperature					Lower heating value of fuel		
kg/kmol 18.661	kg/m^3 0.8325					MJ/kg 44.454		

Table 2 Mole fraction of different species in oxidizer

Species	O_2	N_2	H_2O	CO_2	C_nH_m
Oxidizer volume fraction	99.5	ppm < 100	ppm < 10	ppm < 5	ppm < 20

2.3 Numerical procedure

Numerical simulations have been done by OpenFOAM® software. The ReactingFOAM transient combustion solver has been used to perform simulations The PaSR combustion model of this solver has been used to model the turbulence and chemical reactions interactions. The effect of chemical reactions and flow turbulence are considered in the PaSR model in order to calculate the reaction rates. The P1 and DO models have been used to investigate the effect of radiation heat transfer modeling. In the small optical thickness (less than 1 mm) the DO model is more accurate than P1 model but the simulation speed of the P1 model is much faster than DO model [13]. The absorption and emission coefficients are calculated using the four different models: the WSGGM model, the modified WSGGM model by Yin [14] that was added to the solver, the Grey Mean model, and the use of constant coefficients for calculating the absorption and emission coefficients. The simulations showed the k-ε standard turbulence model with the modified coefficient $C_{1\varepsilon}$ had the closest agreement with the experimental data due to the circular nozzles of air and fuel inlets. Therefore, the $C_{1\varepsilon}$ coefficient has been changed from 1.44 to 1.6 [22]. The effects of modified 2-step WD and 4-step JL mechanisms (modified JL mechanism by Andersen and Yin) have been investigated on the temperature distributions.

The PIMPLE algorithm employed to resolve the coupling of the pressure and velocity. A combination of PISO and SIMPLE algorithms used in this algorithm. The discretization of convection terms performed by second order upwind scheme for the continuity, momentum, and energy equations. The convergence criteria for numerical simulations included: residuals to less than 10^{-6} for all equations in each time step and temperature changes to less than 0.1 K in the time period of 0.05 s in the outlet of furnace.

Table 3 Governing condition on the fuel and oxidizer inlets in oxy-fuel simulation

Flow type	• Variable	• Variable value
Oxidizer flow	• Mass flow rate	• 224.5 kg/h
	• Velocity	• 118.53 m/s
	• Temperature	• 298.15 K
	• Pressure	• 101,369.2 Pa
Fuel flow	• Mass flow rate	• 63 kg/h
	• Velocity	• 114.19 m/s
	• Temperature	• 298.15 K
	• Pressure	• 101,369.2 Pa

3 Governing equations

The governing equations of the problem consist of the mass conservation equation, the momentum conservation equations, the energy conservation equation, and the species conservation equations wich are presented in several reference such as [23]. The chemical mechanism and radiative heat transfer modelling have been considered in connection with combustion model in the present study. In the follwing, the combustion and radiative heat transfer models are explained.

3.1 Combustion modelling

In the averaged equations, it is necessary to model the mean mass reaction rate of species k, $\bar{\dot{\omega}}_k$. Different models have been proposed for this purpose. In this study, PaSR combustion model was used. In this model, the effect of both mixing parameters and chemical kinetics in the combustion process is considered. In the PaSR combustion modeling, each computational cell is divided into two uniformly reactive and non-reactive parts [24, 25].

In addition, the reaction zone acts as a homogeneous mixing reactor (given each species is completely mixed with other species). Based on this, every oscillation can be ignored in chemical source terms calculation [25]. In this method, chemistry effects, large-scale separation, and the effects of micro-mixing is considered, and only the effects of non-uniformity of molecular mixing in the reaction zone is disregard [24]. The average reaction rate for k-th species in the species equation is obtained from Eq. (3).

$$\frac{c_k^1 - c_k^0}{dt} = \overline{\dot{\omega}_r} = \kappa^* \dot{\omega}_k \tag{2}$$

$$\kappa^* = \frac{\tau}{\tau + \tau_{mix}} \tag{3}$$

Where τ and τ_{mix} represent reaction time and micro mixing (eddy break-up) time [24]. In these equations, c^0 is the average concentration at inlet of the cell that may be the initial average concentration of each cell. c is concentration in the reaction zone in the fine structures which is unknown, and c^1 is average concentration of the output from the reaction zone which is equal to the average concentration of total cells. It is calculated as the Eq. (4) in which κ^* is mass fraction of reaction mixture [25].

$$c^1 = \kappa^* c + \left(1 - \kappa^*\right) c^0 \tag{4}$$

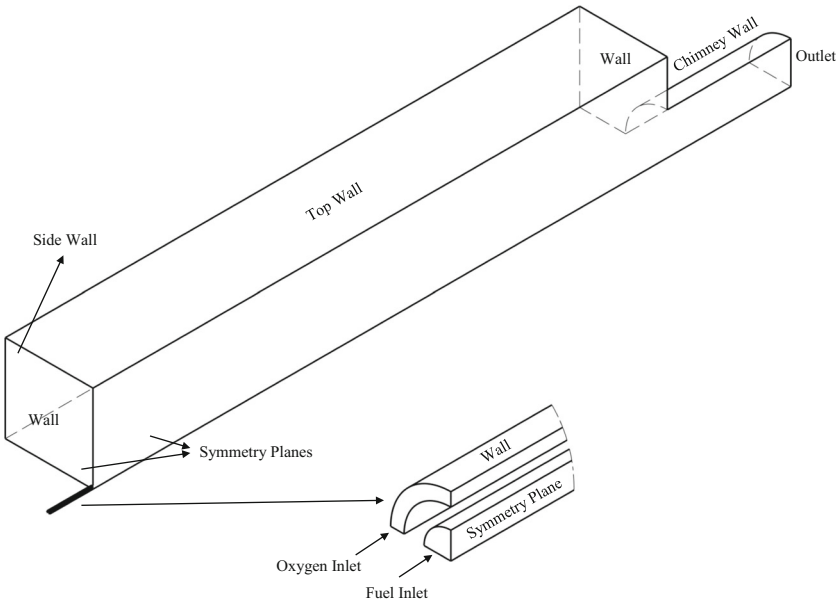

Fig. 2 Boundary condition on the oxy-fuel furnace

If the total time is much larger than the turbulence mixing time ($\tau \gg \tau_{mix}$), it can be concluded that $\kappa^* \approx 1$. In this case, the whole reactor will have reaction. By knowing κ^*, the unknown parameter c eliminates and one can obtain c^1. In general, the choice of τ_{mix} depends on many things, including the flow and the used chemical mechanisms. In the used solver, the following Eq. (5) has been used to calculate the τ_{mix}.

$$\tau_{mix} = C_{mix}\sqrt{\frac{\mu_{eff}}{\bar{\rho}\tilde{\varepsilon}}} \tag{5}$$

Where μ_{eff} is effective viscosity and C_{mix} is a constant coefficient which can have a value of about 0.001–0.3, depending on the flow. The C_{mix} parameter is chosen based on Reynolds number of fuel and oxidizer flow (with increasing of Reynolds number, smaller C_{mix} use in simulations). In this study, $C_{mix} = 0.01$ was used due to high Reynolds number of inlet flows [25]. To calculate the overall reaction time according to the species that have smaller concentrations averaged (limiting species), the relationship (6) is used [26].

Table 4 Different chemical mechanisms used in the present study

Reaction No.	Reaction	Reaction order	A	b	E
Modified Westbrrok-Dryer Mechanism [10]					
1	$CH_4 + 1.5O_2 \rightarrow CO + 2H_2O$	$\frac{d[CH_4]}{dt} = AT^b e^{-E/RT}[CH_4]^{0.7}[O_2]^{0.8}$	5.03×10^{11}	0	2.0×10^8
2	$CO + 0.5O_2 \rightarrow CO_2$	$\frac{d[CO]}{dt} = AT^b e^{-E/RT}[CO][O_2]^{0.25}[H_2O]^{0.5}$	2.24×10^8	0	4.18×10^7
3	$CO_2 \rightarrow CO + 0.5O_2$	$\frac{d[CO_2]}{dt} = AT^b e^{-E/RT}[CO][O_2]^{-0.25}[H_2O]^{0.5}$	1.10×10^{13}	−0.97	3.28×10^8
Modified Jones-Lindstedt Mechanism (Andersen) [9]					
1	$CH_4 + 0.5O_2 \rightarrow CO + 2H_2$	$\frac{d[CH_4]}{dt} = AT^b e^{-E/RT}[CH_4]^{0.5}[O_2]^{1.25}$	4.4×10^{11}	0	1.26×10^8
2	$CH_4 + H_2O \rightarrow CO + 3H_2$	$\frac{d[CH_4]}{dt} = AT^b e^{-E/RT}[CH_4]\,[H_2O]$	3.0×10^8	0	1.26×10^8
3	$H_2 + 0.5O_2 \rightarrow H_2O$	$\frac{d[H_2]}{dt} = AT^b e^{-E/RT}[H_2]^{0.25}[O_2]^{1.5}$	5.69×10^{18}	−1	1.26×10^8
4	$H_2O \rightarrow H_2 + 0.5O_2$	$\frac{d[H_2O]}{dt} = AT^b e^{-E/RT}[H_2]^{-0.25}[O_2]\,[H_2O]$	5.2×10^{19}	−0.877	4.1×10^8
5	$CO + H_2O \leftrightarrow CO_2 + H_2$	$\frac{d[CO]}{dt} = AT^b e^{-E/RT}[CO]\,[H_2O]$	2.75×10^9	0	8.4×10^7
Modified Jones-Lindstedt Mechanism (Yin) [10]					
1	$CH_4 + 0.5O_2 \rightarrow CO + 2H_2$	$\frac{d[CH_4]}{dt} = AT^b e^{-E/RT}[CH_4]^{0.5}[O_2]^{1.25}$	4.4×10^{11}	0	1.26×10^8
2	$CH_4 + H_2O \rightarrow CO + 3H_2$	$\frac{d[CH_4]}{dt} = AT^b e^{-E/RT}[CH_4]\,[H_2O]$	3.0×10^8	0	1.26×10^8
3	$H_2 + 0.5O_2 \leftrightarrow H_2O$	$\frac{d[H_2]}{dt} = AT^b e^{-E/RT}[H_2][O_2]^{0.5}$	5.69×10^{11}	0	1.465×10^8
4	$CO + H_2O \leftrightarrow CO_2 + H_2$	$\frac{d[CO]}{dt} = AT^b e^{-E/RT}[CO]\,[H_2O]$	2.75×10^8	0	8.36×10^7

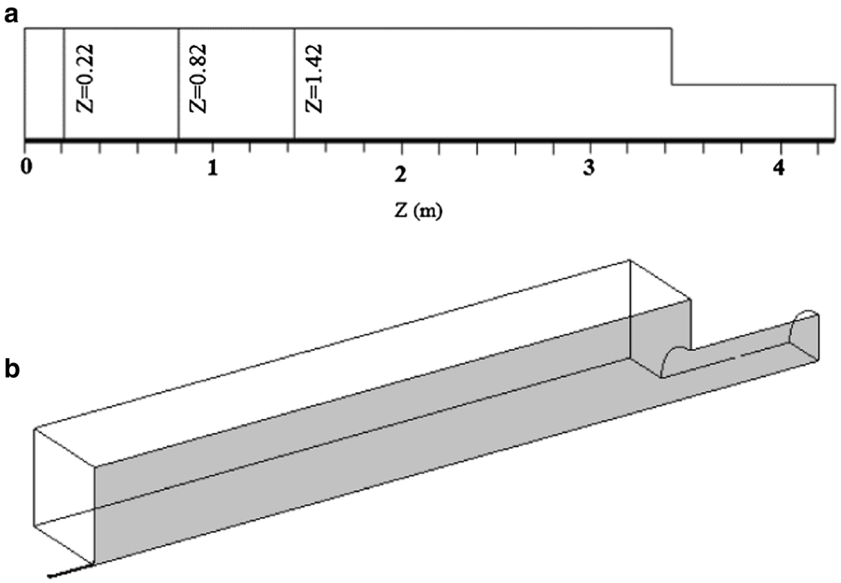

Fig. 3 **a** Cross-sections of furnace in order presentation of the results, **b** Considered plane in order to presented contours

$$\frac{1}{\tau} = \max\left\{\frac{-\widetilde{\omega}_{\mathrm{Fuel}}}{\overline{\rho}}, \frac{-\widetilde{\omega}_{\mathrm{O_2}}}{\overline{\rho}}\right\} \tag{6}$$

3.2 Radiative heat transfer modelling

Radiative heat transfer is an important heat transfer mechanism due to high gas temperature. Therfore, radiative heat transfer calculation of high temperature combustion product is essential in the furnaces and boilers. The source term of radiative heat transfer should be modeled in the numerical simulations.

The many methods exist for the modelling of radiative heat transfer from high temperature gas. These models have different precision and run time. More precise methods require a smaller computational grid and division of the numerical domain into several sections. The choice of method should be based on the type of combustion conditions with more precision and fewer numerical simulations time. The P1 and DO radiative heat transfer models has been paid more attention in the recent years. These methods are tools for converting the RTE into a set of PDE equations. The basic idea in the P1 model is that the intensity in a participating medium can be represented as a rapidly converging series whose terms are based on orthogonal spherical harmonics. This method is from PN approximation family method for RTE calculation and suitable only for isotropic environments in terms of radiation intensity. For other environments, it requires the use of higher order precision methods with very high mathematical complexity [13].

DO model is based on discrete the directional variations of radiation intensity. In this method, the solution of RTE is obtained by solving the transfer equation for a set of discrete directions, which includes the full range of solid angles (equal to 4π). DO model solve the RTE equations proportional to the number of discrete directions. This model is one of the most accurate methods for solving the RTE. DO model can predict the temperature distribution in wider range of optical thickness unlike P1 method. In addition to, the non grey assumption for the calculation of emission and absorption model is provided only in DO model. However, time cost of DO model is more than P1 radiative heat transfer model [13].

3.3 Chemical mechanism

Chemical mechanism has the special role in the accuracy and run time of combustion simulations. The global kinetics with suitable coefficient can lead to correct prediction of temperature distribution in the burners and furnaces. These chemical

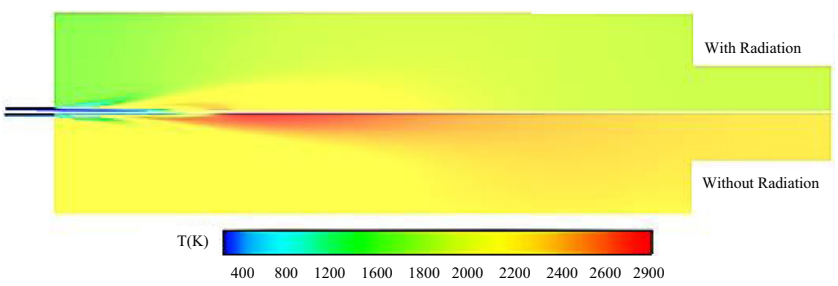

Fig. 4 Effect of considering radiation on the numerical simulation results

mechanisms have very little simulation time in comparison with detailed and skeletal mechanisms such as GRI or DRM. The modified WD, modifid JL (by Andersen), and the modified JL (by Yin) chemical mechanisms are used in the present study, as indicated in the Table 4. Difference in these mechanism is in the number of species, and reactions and the coefficient of reaction used in the Arenihus equation for calculation of the reaction rates.

4 Results and discussion

The results of simulations are presented in this section. In order to investigation the grid independency of the results, the numerical grids with 570,000, 1,100,000 and 2,200,000 cells are used. The obtained results show that using of 1,100,000 cells lead to the independence of the results from the numerical grid.

The results of simulations are expressed as curves on certain axial distances and in the form of contours on the symmetry plane. The profiles are at 22, 82 and 142 cm from the beginning of the furnace on the symmetry plane are shown in Fig. 3a. The contours are in a plane that is shown in Fig. 3b.

4.1 Effect of the radiative heat transfer model

The effect of applying radiation on the temperature distribution inside the furnace is shown in Fig. 4 (the DO radiation model and WSGGM model used in these figures). Due to the reduction of the cross-section area at the end of furnace, there is an intense recirculation of combustion products. This recirculation causes that the high temperature combustion products (extensively included H_2O and CO_2 (to be released throughout the furnace and the temperature of furnace increase away from the flame formation regions. This raises the importance of considering radiative heat transfer according to Fig. 4 throughout of furnace.

The effect of radiation exposure on the temperature distribution for modified JL mechanisms is investigated in Fig. 5a to c. The results were compared with the experimental data. Considering the radiation led to reduction of the average temperature by 350 K which indicates the importance of radiation in the oxy-fuel combustion. Another important issue in

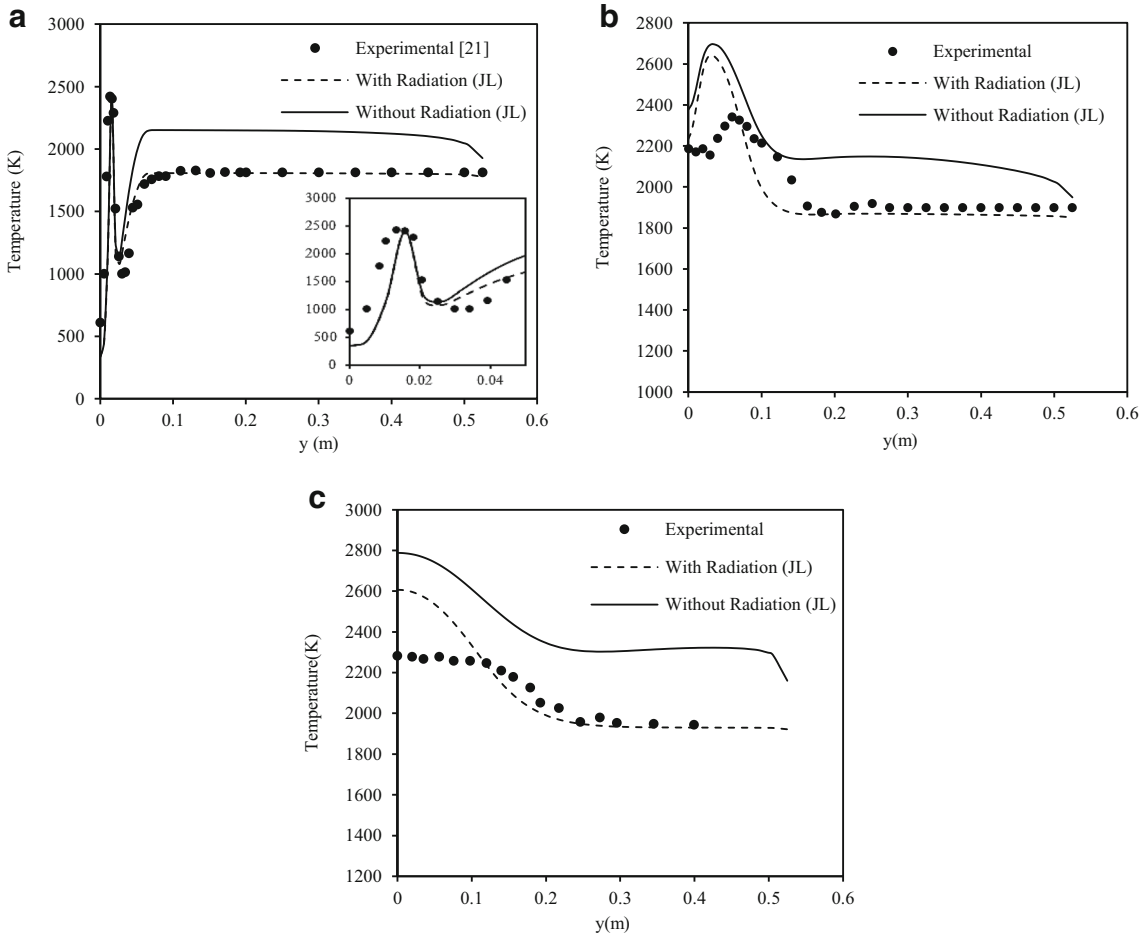

Fig. 5 Effect of applying radiation on the temperature distribution: **a** 22 cm distance from inlet furnace; **b** 82 cm distance from inlet furnace; **c** 142 cm distance from inlet furnace

examining the variation of maximum temperature with radiation exposure that the radiation reduces the maximum temperature about 500 K. The effect of radiation in this situation is not only due to the high temperature of the combustion gases in the oxy-fuel combustion, but also because of the main combustion products H_2O and CO_2 which have much higher absorption and emission coefficients than nitrogen. This makes radiation heat transfer mechanism as an important part in the oxy-fuel combustion.

In this study, the two models of radiation P1 and DO using the grey gases model were used to modelling of the radiative heat transfer. The results of simulations are shown in Fig. 6a to c. According to the results, there is a slight difference between DO and P1 radiation model results in the calculation of temperature. The middle size of furnace leads to thin optical thickness in which that P1 and DO models don't have much difference. The DO model shown the better accuracy of the results (average of about 2%) in the different cross-sections. This issue is one of the challenges in P1 model due to the overprediction of radiation heat loss.

4.2 Effect of the evaluated of radiation coefficients model

Oxy-fuel combustion products contain H_2O and CO_2 which have different radiation properties than N_2. CO_2 and H_2O have emission and absorption coefficients which changed with temperature and wavelength significantly. Therefore, the choice of radiation coefficient calculation method can provide acceptable accuracy with appropriate time cost. Four method with different run time and accuracy for absorption and emission calculation were used in the present study. These methods include constant coefficients, grey mean, WSGGM, and modified WSGGM. In the constant coefficients method, the absorption and emission coefficients of species are used at 1800 K which is the average temperature in the IFRF furnace. In the grey mean method, the sixth order polynomial for each combustion species is used to calculate the absorption and emission coefficients. The WSGGM and modified WSGGM methods are based on the Smith [16] and Yin [15] studies. The WSGGM method uses the weighted sum of emission and absorption coefficients and these coefficients which are

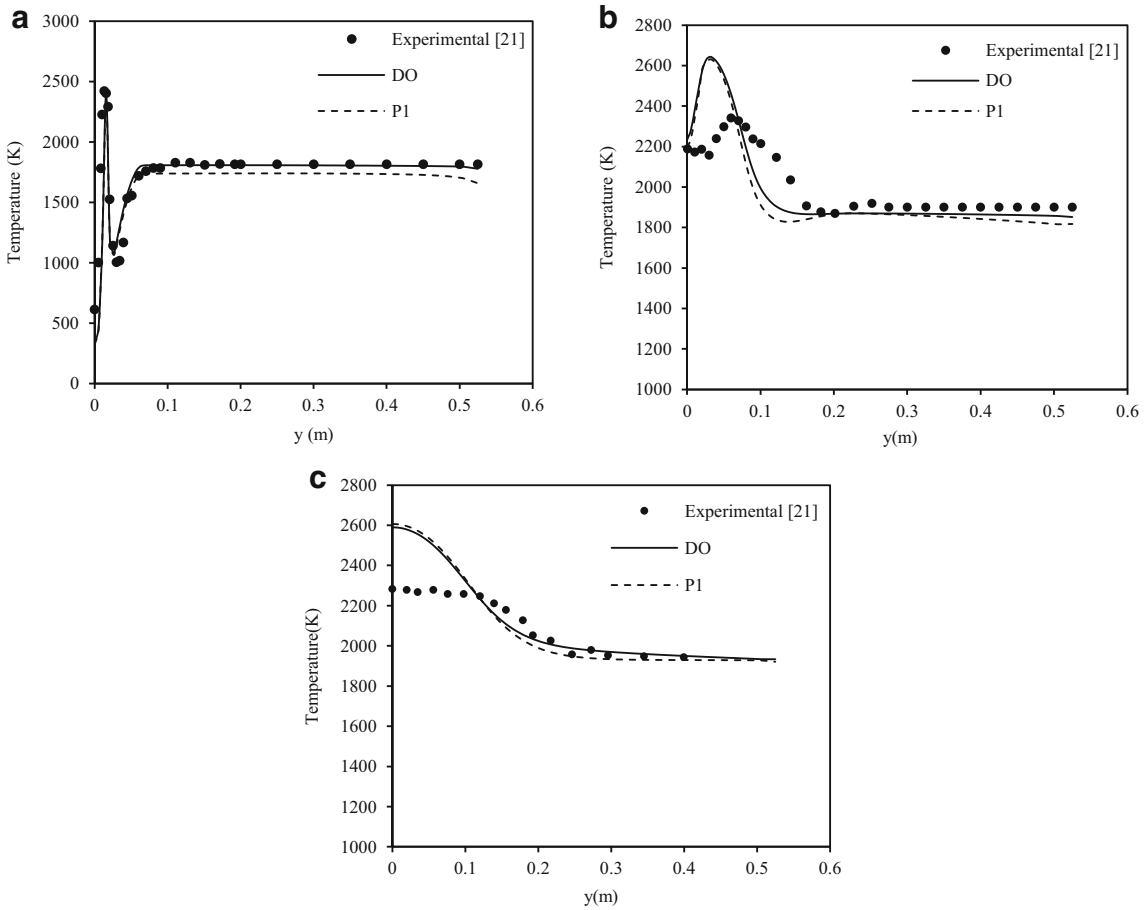

Fig. 6 Effect of radiation heat transfer model on the temperature: **a** 22 cm distance from inlet furnace; **b** 82 cm distance from inlet furnace; **c** 142 cm distance from inlet furnace

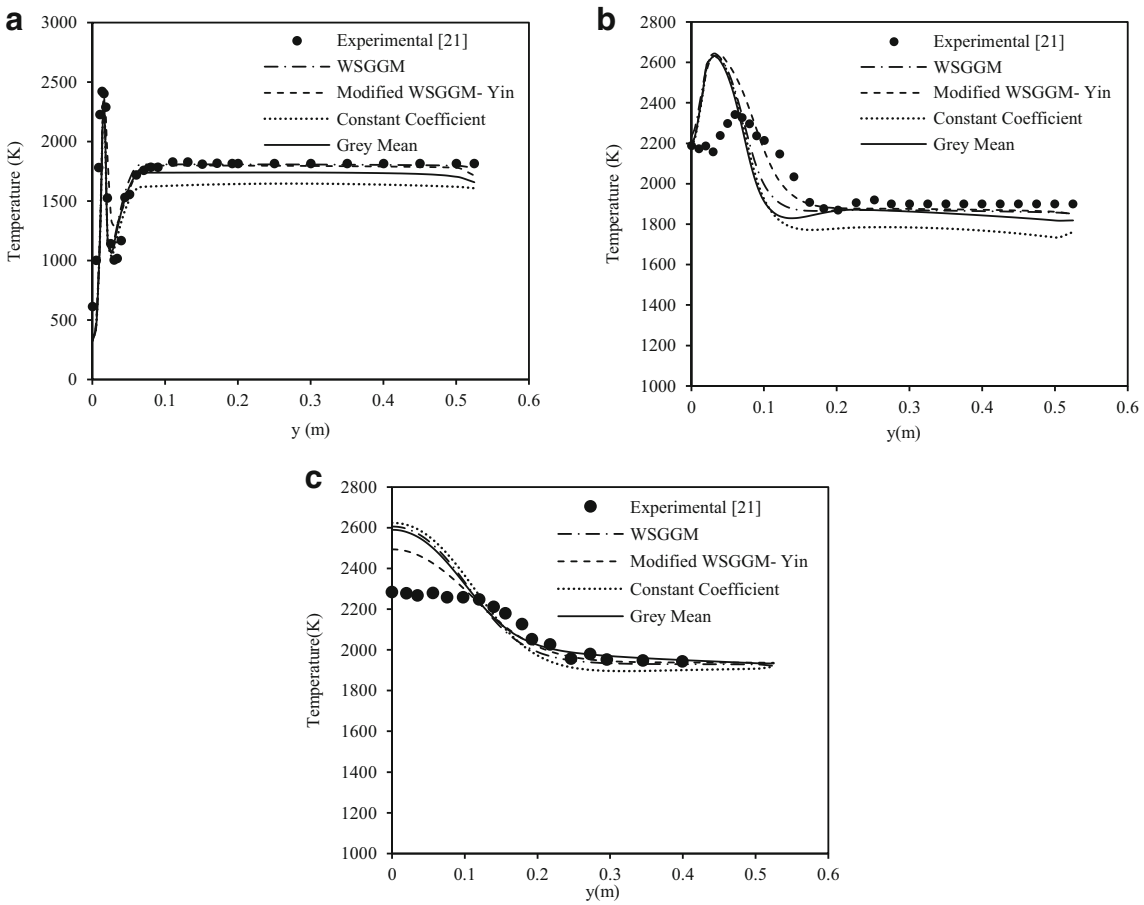

Fig. 7 Effect of radiation coefficient on the temperature at different sections of furnace: **a** 22 cm distance from inlet furnace; **b** 82 cm distance from inlet furnace; **c** 142 cm distance from inlet furnace

constant at the different wavelength. The modified WSGGM model uses wavelength dependent coefficients for the calculation of radiative coefficients.

Temperature variations in the furnace for different methods of calculating radiation coefficients using the DO model and modified JL kinetics are shown in Fig. 7. The results show that the method of constant coefficients has a significant difference compared to other methods. This difference is evident in high temperature regions since that constant coefficients taking into account at 1800 K. The comparison between the WSGGM, grey mean and modified WSGGM methods also show that the results obtained from these methods have little difference. This result is accordance with the results from reference [10] for WGGGM and modified WSGGM methods. The modified WSGGM method offers less error than WSGGM and grey mean models due to the use of wavelength dependent coefficients for the calculation of emission and absorption coefficients.

4.3 Effect of chemical mechanism

The temperature distribution for different kinetics is shown in Fig. 8a to c. The correction of the reaction rate coefficients and the consideration of one additional reaction in the modified 2-step WD mechanism. However, modified 2-step WD mechanism still predicts the maximum temperature more than the experimental data in all sections significantly (2-step kinetics relative to the 4-step kinetics at the site of the flame formation predicts considerably more temperature values). The H_2 species doesn't exist in the 2-step modified WD mechanism. Therefore, this kinetic can't include the dissociation reaction of H_2O to H_2 which is an endothermic reaction which cause the reduction of the maximum flame temperature. In addition to, at high temperature condition, consumption of CO_2 into CO may start by atomic hydrogen. As mentioned, H_2 does not exist in the modified 2-step WD mechanism; Hence, reaction rate of CO_2 to CO reduced and lead to the high temperature prediction in numerical simulations.

The predicted temperature for modified 2-step mechanism at 82 and 142 cm show a larger error than the 22 cm cross-section, due to the flame spreading along the furnace. In fact, in the flame formation region (high temperature region of the furnace), dissociation reactions are very important in predicting the temperature. Hence, 4-step kinetics results are better than the 2-step kinetics in the high temperature region. It should also be noted that in Fig. 8a, the difference between

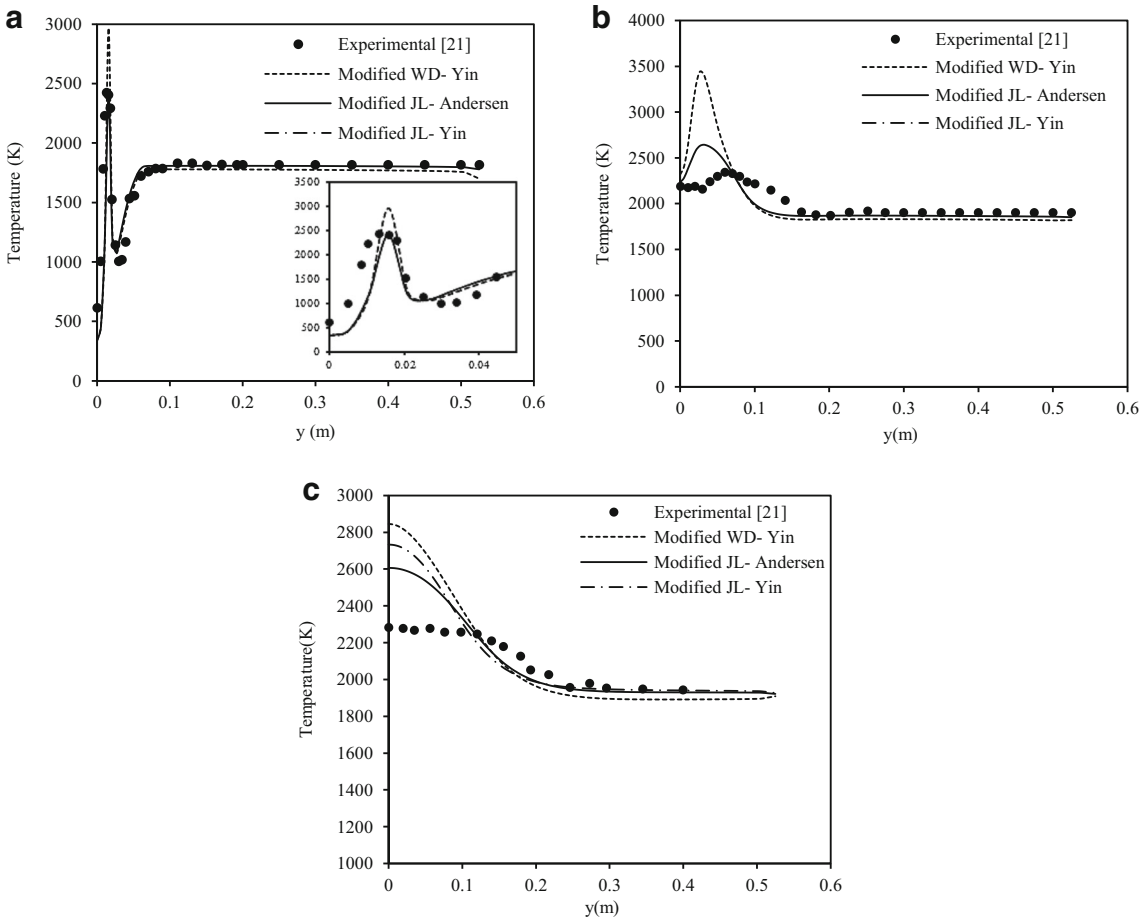

Fig. 8 Effect of different reduced chemical kinetics on the temperature distribution: **a** 22 cm distance from inlet furnace; **b** 82 cm distance from inlet furnace; **c** 142 cm distance from inlet furnace

chemical kinetics in the prediction of temperature for the middle section of furnace; according to this figure, the prediction of maximum temperature in the modified 2-step mechanism has high error.

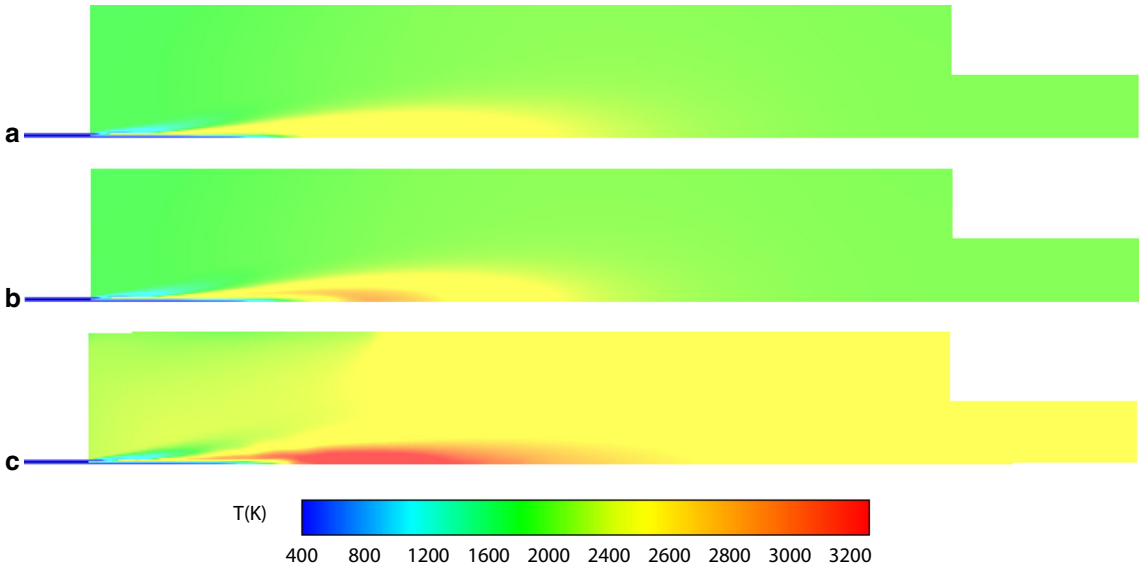

Fig. 9 Temperature contours with different chemical kinetics: **a** modified 4-step Andersen kinetic; **b** modified 4-step Yin kinetic; **c** modified 2-step WD kinetic

In Fig. 9a to c, two different modified 4-step kinetics are also studied. According to the obtained results at different sections, the Andersen kinetic results show better results than Yin kinetics at different intervals, contrary to the results obtained in reference [10]. In this reference, the EDC combustion model was used to simulate the IFRF furnace. The conclusion of this study have indicated that the modified kinetics by them has better results than Andersen's kinetics, which in the present study show the opposite.

Figure 9a to c show the comparison between the temperature distribution of the three kinetics. The maximum temperature in the 2-step Yin kinetics is more than 3400 K, which is much higher than the maximum predicted by the 4-step kinetics. The difference is related to the dissociation reactions. In addition to, the maximum temperature predicted with modified 4-step Yin kinetic is over 2900 K, which is approximately equivalent to the adiabatic flame temperature predicted with equilibrium calculations by the GRI-Mech 3.0 mechanism [10]. The maximum temperature obtained by 4-step Andersen kinetic is more than 2600 K. The maximum flame temperature should be less than the adiabatic flame temperature due to existence of non-equilibrium conditions and irreversibility in real situations, which is discussed only in modified 4-step Andersen kinetic.

5 Conclusion

In this study, the effect of radiation exposure, radiation model, calculation method of the adsorption and emission coefficients as well as effect of the chemical mechanism were studied. The results indicated the importance of radiative heat transfer in oxy-fuel combustion, which has a significant impact on the distribution of temperature. Due to the high temperature of the gases, the P1 model predicts the amount of radiation loss to be slightly more than the experiments. The use of the modified WSGGM, WSGGM and grey mean models to calculate the absorption and emission coefficients of oxy-fuel combustion lead to an acceptable prediction of the temperature than the other models. Modified 2-step WD and 4-step JL mechanisms with correction of reaction order, activation energy and pre-exponent factors were compared for investigation of chemical mechanism effects. Different 4-step chemical mechanisms used do not have significant effect on the temperature distribution. 4-step chemical mechanism have lower maximum temperature and more precision than modified 2-step WD mechanism due to consideration of dissociation reactions (dissociation of H_2O to H_2 and dissociation of CO_2 to CO due to existence of atomic hydrogen).

References

1. Demirbas A (2005) Potential applications of renewable energy sources, biomass combustion problems in boiler power systems and combustion related environmental issues. Prog Energy Combust Sci 31(2):171–192
2. Scheffknecht G, Al-Makhadmeh L, Schnell U, Maier J (2011) Oxy-fuel coal combustion—a review of the current state-of-the-art. Int J Greenh Gas Cont 5:S16–S35
3. Metz B (2005) Carbon dioxide capture and storage: special report of the intergovernmental panel on climate change. Cambridge University Press, Cambridge
4. Rackley SA (2017) Carbon capture and storage. Butterworth-Heinemann, Oxford
5. Prieler R, Demuth M, Spoljaric D, Hochenauer C (2014) Evaluation of a steady flamelet approach for use in oxy-fuel combustion. Fuel 118:55–68
6. Prieler R, Mayr B, Demuth M, Spoljaric D, Hochenauer C (2015) Application of the steady flamelet model on a lab-scale and an industrial furnace for different oxygen concentrations. Energy 91: 451–464
7. Westbrook CK, Dryer FL (1984) Chemical kinetic modeling of hydrocarbon combustion. Prog Energy Combust Sci 10(1):1–57
8. Jones W, Lindstedt R (1988) Global reaction schemes for hydrocarbon combustion. Combust Flame 73(3):233–249
9. Andersen J, Rasmussen CL, Giselsson T, Glarborg P (2009) Global combustion mechanisms for use in CFD modeling under oxy-fuel conditions. Energy Fuel 23(3):1379–1389
10. Yin C, Rosendahl LA, Kær SK (2011) Chemistry and radiation in oxy-fuel combustion: a computational fluid dynamics modeling study. Fuel 90(7):2519–2529
11. Chen L, Ghoniem AF (2014) Modeling CO2 chemical effects on CO formation in oxy-fuel diffusion flames using detailed, quasi-global, and global reaction mechanisms. Combust Sci Technol 186(7):829–848
12. Howell JR, Menguc MP, Siegel R (2010) Thermal radiation heat transfer. CRC press, Boca Raton
13. Modest MF (2013) Radiative heat transfer. Academic press, Cambridge
14. Yin C (2013) Refined weighted sum of grey gases model for air-fuel combustion and its impacts. Energy Fuel 27(10):6287–6294
15. Yin C, Johansen LC, Rosendahl LA, Kær SK (2010) New weighted sum of grey gases model applicable to computational fluid dynamics (CFD) modeling of oxy− fuel combustion: derivation, validation, and implementation. Energy Fuel 24(12):6275–6282
16. Smith T, Shen Z, Friedman J (1982) Evaluation of coefficients for the weighted sum of grey gases model. J Heat Transf 104(4):602–608
17. Wheaton Z, Stroh D, Krishnamoorthy G, Sami M, Orsino S, Nakod P (2013) A comparative study of grey and non-grey methods of computing gas absorption coefficients and its effect on the numerical predictions of oxy-fuel combustion. Journal of the International Flame Research Foundation 1–14
18. Andersson K, Johnsson F (2007) Flame and radiation characteristics of gas-fired O2/CO2 combustion. Fuel 86(5–6):656–668
19. Brink A, Hupa M, Breussin F, Lallemant N, Weber R (2000) Modeling of oxy-natural gas combustion chemistry. J Propuls Power 16(4):609–614
20. Lallemant N, Dugue J, Weber R (1997) Analysis of the experimental data collected during the OXYFLAM-1 and OXYFLAM-2 experiments. IFRF Doc F 85
21. Bollettini U, Breussin F, Lallemant N, Weber R (1997) Mathematical modeling of oxy-natural gas flames. IFRF Doc:F85

22. Christo FC, Dally BB (2005) Modeling turbulent reacting jets issuing into a hot and diluted coflow. Combust Flame 142(1–2):117–129
23. Poinsot T, Veynante D (2005) Theoretical and numerical combustion. RT Edwards, Philadelphia
24. Chomiak J, Karlsson A (1996) Flame liftoff in diesel sprays. In: Symposium (International) on Combustion. vol 2. Elsevier, p 2557–2564
25. Nordin P (2001) Complex chemistry modeling of diesel spray combustion. Chalmers University of Technology, Gothenburg
26. Guessab A (2013) RANS simulation of methane diffusion flame comparison of two chemical kinetics mechanisms. J Phys Sci Appl 3(2):400–408